

To Professor Mutsuo Oka  
on the occasion  
of his 60th birthday

## ON THE CONTACT STRUCTURE OF A CLASS OF REAL ANALYTIC GERMS OF THE FORM $f\bar{g}$

MASAHARU ISHIKAWA

ABSTRACT. It is known that the argument map  $f\bar{g}/|f\bar{g}| : S_\varepsilon^3 \setminus L_{f\bar{g}} \rightarrow S^1$  of a real analytic germ  $(f\bar{g}, O) : (\mathbb{C}^2, O) \rightarrow (\mathbb{C}, 0)$  defines a locally trivial fibration under a certain condition. In this article we prove that if it is a fibration and  $f$  and  $g$  are of the form  $f = x^p + y^q$  and  $g = x^r + y^s$  then the compatible contact structure is always overtwisted. In particular, it follows that the monodromy of this fibration contains at least one negative Dehn twist.

### 1. INTRODUCTION

Let  $(h, O) : (\mathbb{C}^{n+1}, O) \rightarrow (\mathbb{C}, 0)$  be a holomorphic germ with  $h(O) = 0$ , where  $O$  is the origin of  $\mathbb{C}^{n+1}$ . The intersection  $L_h$  of  $h^{-1}(0)$  with a sphere  $S_\varepsilon^{2n+1}$  centered at  $O \in \mathbb{C}^{n+1}$  with sufficiently small radius  $\varepsilon > 0$  is called the *link* of  $(h, O)$ . In [13], J. Milnor proved that the argument map  $h/|h| : S_\varepsilon^{2n+1} \setminus L_h \rightarrow S^1$  is a locally trivial fibration and that, under a certain condition, a real analytic germ also defines a locally trivial fibration over  $S^1$ . There are several studies concerning this condition, see for instance [23, Ch. VII and VIII] and the references therein.

In [17], A. Pichon studied real analytic germs of the form  $(f\bar{g}, O)$ , where  $(f, O)$  and  $(g, O)$  are holomorphic germs from  $(\mathbb{C}^2, O)$  to  $(\mathbb{C}, 0)$  with isolated singularities and with no common branches. Here  $\bar{g}$  represents the conjugation of  $g$ . In particular, a condition for the link  $L_{f\bar{g}}$  to be fibred is given in terms of the multiplicities on resolution graphs of  $(f, O)$  and  $(g, O)$ . Then she and J. Seade proved in [18] that  $f\bar{g}/|f\bar{g}| : S_\varepsilon^3 \setminus L_{f\bar{g}} \rightarrow S^1$  is a locally trivial fibration if and only if  $(f\bar{g}, O)$  satisfies the fibrability condition in [17] in more general context. In [3], A. Bodin and Pichon studied the multilinks of meromorphic functions of the form  $f/g$  and represented the fibrability condition for  $(f\bar{g}, O)$  in terms of special fibres of  $f/g$ .

Let  $M$  be an oriented, closed, smooth 3-manifold. A fibration from a link complement of  $M$  to  $S^1$  is called an *open book decomposition* of  $M$ . For instance, the fibration  $f\bar{g}/|f\bar{g}| : S_\varepsilon^3 \setminus L_{f\bar{g}} \rightarrow S^1$  is an open book decomposition of  $S_\varepsilon^3$ . The idea of a contact structure compatible with an open book decomposition was first introduced by W.P. Thurston and H. Winkelnkemper in [24], where they proved that every open book decomposition

---

2000 *Mathematics Subject Classification*. Primary: 57M50, Secondary: 57R17, 32S55, 57M25.

*Key words and phrases*. contact structure, open book decomposition, quasipositive surface.

This work is supported by MEXT, Grant-in-Aid for Young Scientists (B) (No. 19740029).

admits a compatible contact structure. Moreover, it is known by E. Giroux that if two contact structures are compatible with the same open book decomposition then they are contactomorphic, i.e., there exists an automorphism which maps one contact structure to the other [8]. This means that the compatible contact structure is an invariant of the open book decomposition up to contactomorphism. Hence, to make a classification of fibred links in  $M$ , determining their compatible contact structures is important.

There are roughly two kinds of contact structures on 3-manifolds: tight contact structures and overtwisted ones. Let  $(M, \xi)$  denote the manifold  $M$  equipped with a contact structure  $\xi$ , called a *contact manifold*. A disk  $D$  in  $(M, \xi)$  is called *overtwisted* if  $D$  is tangent to  $\xi$  at each point on the boundary of  $D$ . If  $(M, \xi)$  has an overtwisted disk then we say  $\xi$  is *overtwisted* and otherwise we say  $\xi$  is *tight*. The classification of contact structures on  $S^3$  up to contactomorphism had been done by Y. Eliashberg in [5] and [7]. In particular, he proved that  $S^3$  admits a unique tight contact structure up to contactomorphism, which is called the *standard contact structure*.

In this paper, we study real analytic germs  $(f\bar{g}, O)$  given by

$$f = x^p + y^q \quad \text{and} \quad g = x^r + y^s,$$

where  $p, q, r, s \in \mathbb{N}$  and  $(f, O)$  and  $(g, O)$  are holomorphic germs from  $(\mathbb{C}^2, O)$  to  $(\mathbb{C}, 0)$  having no common branches. It follows from [17, Corollary 2.2] and [18, Theorem 2.1] that  $f\bar{g}/|f\bar{g}| : S_\varepsilon^3 \setminus L_{f\bar{g}} \rightarrow S^1$  is a locally trivial fibration if and only if either

- (1)  $p \neq r$  and  $q \neq s$ ,
- (2)  $p = r > 1$ ,  $q \neq s$  and  $\min\{q, s\} = 1$ ,
- (3)  $p \neq r$ ,  $q = s > 1$  and  $\min\{p, r\} = 1$ , or
- (4) at least three of  $p, q, r, s$  are 1,

see Lemma 3.1 below. The main result is the following:

**Theorem 1.1.** *Let  $(f, O)$  and  $(g, O)$  be holomorphic germs given by  $f = x^p + y^q$  and  $g = x^r + y^s$  having no common branches. Suppose  $f\bar{g}/|f\bar{g}| : S_\varepsilon^3 \setminus L_{f\bar{g}} \rightarrow S^1$  is a locally trivial fibration. Then its compatible contact structure is overtwisted.*

It is known by A. Loi and R. Piergallini in [11], combined with “fillable  $\Rightarrow$  tight” in [6], that if the monodromy of an open book decomposition is represented as a product of positive Dehn twists then the compatible contact structure is tight. By contraposition, we have the following corollary:

**Corollary 1.2.** *The monodromy of the fibration  $f\bar{g}/|f\bar{g}|$  in Theorem 1.1 contains at least one negative Dehn twist.*

Here is a remark concerning the contact structures compatible with the fibrations of a holomorphic germ  $(f, O)$  and its conjugation  $(\bar{f}, O)$ . It is well-known that the monodromy of the Milnor fibration of  $(f, O)$  is represented as a product of positive Dehn twists. Hence the Milnor fibration is compatible with the standard contact structure on  $S_\varepsilon^3$ . The fibration of the germ  $(\bar{f}, O)$  is also represented as a product of positive Dehn twists because  $(x, y) \mapsto (\bar{x}, \bar{y})$  does not change the orientation of  $S_\varepsilon^3$ , reverse the argument  $e^{i \arg f}$  to  $e^{-i \arg f}$  in the target of the fibration, and reverse the orientation of the fibre surface. Hence, to have a fibration compatible with an overtwisted contact structure, a mixture of  $(f, O)$  and  $(\bar{g}, O)$  is necessary.

This paper is organized as follows. In Section 2 we give the definitions of open book decompositions and compatible contact structures, and also introduce quasipositive surfaces in  $S^3$  and relation between contact structures and quasipositive surfaces. In Section 3 we calculate the Euler characteristic of the fibre surface of  $f\bar{g}/|f\bar{g}| : S_\epsilon^3 \setminus L_{f\bar{g}} \rightarrow S^1$ . The proof of Theorem 1.1 is written in Section 4. In Section 5 we make a few comments on the case where  $f$  and  $g$  are Newton non-degenerate. Finally, in Section 6, we show that the same conclusion is obtained in the case where the real analytic germ is of the form  $(xy(x^p + y^q), O)$ .

This work is motivated by a question in a talk of Anne Pichon in Luminy, May, 2006. The author would like to thank her for explaining her works concerning the structure of the fibration  $f\bar{g}/|f\bar{g}| : S_\epsilon^3 \setminus L_{f\bar{g}} \rightarrow S^1$ . He is also grateful to Sebastian Baader for useful comments and discussions on quasipositive surfaces.

## 2. CONTACT STRUCTURES COMPATIBLE WITH OPEN BOOKS

An open book decomposition of a closed, oriented, smooth 3-manifold is the following. Let  $F$  be a compact, oriented, smooth 2-dimensional manifold with boundary  $\partial F$  and  $\phi$  an automorphism of  $F$  which is the identity on  $\partial F$ . If a closed, oriented, smooth 3-manifold  $M$  can be obtained from  $F \times [0, 1]$  by identifying  $(\phi(x), 0)$  and  $(x, 1)$  for  $x \in F$  and  $(y, 0)$  and  $(y, t)$  for  $y \in \partial F$  and all  $t \in [0, 1]$ , then we say that  $M$  has an *open book decomposition*. The manifold  $F$  is called a *fibre surface*,  $\partial F$  is the *binding* and  $\phi$  is the *monodromy diffeomorphism*. Note that the binding is also called a *fibred link* in  $M$ .

A *contact structure* on  $M$  is the 2-plane field given by the kernel of a 1-form  $\alpha$  satisfying  $\alpha \wedge d\alpha \neq 0$  everywhere on  $M$ . By changing the orientation of  $M$  if necessary, we assume  $\alpha \wedge d\alpha > 0$ .

**Definition 2.1.** An open book decomposition of  $M$  is said to be *compatible* with a contact structure  $\xi = \ker \alpha$  on  $M$  if

- the fibred link of the open book decomposition is transverse to  $\xi$ ;
- $d\alpha$  is a volume form on each fibre surface;
- the orientation of the fibred link coincides with that of  $\xi$  determined by  $\alpha$ .

Two contact manifolds  $(M_1, \xi_1)$  and  $(M_2, \xi_2)$  are said to be *contactomorphic* if there exists a diffeomorphism  $\varphi : M_1 \rightarrow M_2$  such that  $d\varphi : TM_1 \rightarrow TM_2$  satisfies  $d\varphi(\xi_1) = \xi_2$ . As mentioned in the introduction, Thurston and Winkelnkemper proved that every open book decomposition admits a compatible contact structure [24] and Giroux proved that if two contact structures are compatible with the same open book decomposition then they are contactomorphic [8]. The 3-sphere  $S^3$  admits a unique tight contact structure [7], called the *standard contact structure*, and a unique overtwisted contact structure in each homotopy class of 2-plane fields on  $S^3$  [5].

The standard contact structure on  $S^3$  is characterized by quasipositive surfaces, which we now introduce. A link is called *quasipositive* if it has a diagram which is the closure of a product of conjugates of the positive generators of the braid group. If the product consists only of words of the form

$$\sigma_{i,j} = (\sigma_i \cdots \sigma_{j-2})\sigma_{j-1}(\sigma_i \cdots \sigma_{j-2})^{-1}$$

then the link obtained as its closure is called *strongly quasipositive*. Let  $b$  be the braid index of a braid diagram of a strongly quasipositive link. The link spans a canonical Seifert surface consisting of  $b$  copies of disjoint parallel disks with a band for each  $\sigma_{i,j}$ , see for example Figure 1. Such a diagram of a Seifert surface is called a *quasipositive diagram* and a Seifert surface is said *quasipositive* if it has a quasipositive diagram.

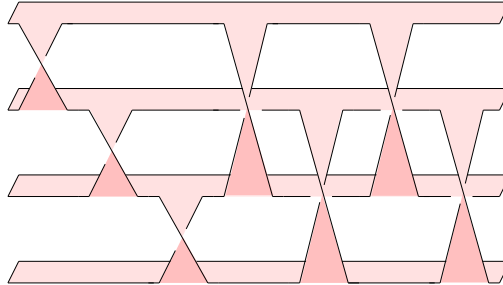


FIGURE 1. An example of quasipositive surface.

The notion of a quasipositive link was introduced by L. Rudolph in [19] and, in the subsequent studies, he found many interesting properties of quasipositive links and surfaces, including deep relation to contact geometry, see for instance [21, 22] and the references therein.

The next theorem gives a useful characterization of the standard contact structure on  $S^3$ .

**Theorem 2.2** (M. Hedden [9], S. Baader-I [2]). *An open book decomposition of  $S^3$  is compatible with the standard contact structure if and only if the fibre surface is quasipositive.*

Therefore, to prove that a fibration is compatible with an overtwisted contact structure, it is enough to prove that the fibre surface is not quasipositive.

We close this section with introducing a lemma which is useful to prove that a given fibre surface is not quasipositive. Let  $\gamma$  be a simple closed curve on an oriented surface  $S$  in  $S^3$ . If  $\gamma$  does not bound a disk in  $S$  then it is called *essential*. A small, compact collar neighborhood  $A(\gamma)$  of  $\gamma$  in  $S$  is an embedded annulus. We orient the two boundary components of  $A(\gamma)$  according to the orientation of  $S$  and denote the linking number of these two oriented boundaries by  $\ell(\gamma, S)$ .

**Lemma 2.3.** *Let  $\gamma$  be an essential, simple closed curve on a quasipositive surface  $S$  and suppose that  $\gamma$  is a trivial knot in  $S^3$ . Then  $\ell(\gamma, S) > 0$ .*

*Proof.* A subsurface  $T$  of a quasipositive surface  $S$  is called *full* if each simple closed curve on  $T$  which bounds a disk in  $S$  already bounds a disk in  $T$ . In [20], Rudolph proved that a full subsurface of a quasipositive surface is quasipositive. Since  $\gamma$  is essential,  $A(\gamma)$  is quasipositive. It is well-known that an unknotted annulus is quasipositive if and only if the linking number of the two oriented boundaries is strictly positive. This can be proved, for example, by combining [2, Lemma 6.1] with the fact that the Thurston-Bennequin invariant of a trivial knot is at most  $-1$ . Thus we have  $\ell(\gamma, S) > 0$ .  $\square$

## 3. THE EULER CHARACTERISTIC OF THE FIBRE SURFACE

In this section we determine the Euler characteristic of the fibre surface of the fibration  $f\bar{g}/|f\bar{g}| : S_\varepsilon^3 \setminus L_{f\bar{g}} \rightarrow S^1$ .

**Lemma 3.1.** *Let  $(f, O)$  and  $(g, O)$  be holomorphic germs given by  $f = x^p + y^q$  and  $g = x^r + y^s$  having no common branches. Then the argument map  $f\bar{g}/|f\bar{g}| : S_\varepsilon^3 \setminus L_{f\bar{g}} \rightarrow S^1$  is a locally trivial fibration if and only if either*

- (1)  $p \neq r$  and  $q \neq s$ ,
- (2)  $p = r > 1$ ,  $q \neq s$  and  $\min\{q, s\} = 1$ ,
- (3)  $p \neq r$ ,  $q = s > 1$  and  $\min\{p, r\} = 1$ , or
- (4) at least three of  $p, q, r, s$  are 1.

In the case it is a fibration, the Euler characteristic  $\chi(F)$  of the fibre surface  $F$  is given by

$$\chi(F) = \begin{cases} |p-r|(1-q) + |q-s|(1-r) & \text{if } p/q \geq r/s, \\ |p-r|(1-s) + |q-s|(1-p) & \text{if } p/q < r/s. \end{cases}$$

*Proof.* We will present the resolution graphs of  $(f, O)$  and  $(g, O)$  and apply [17, Corollary 2.2]. The data of the resolution graphs can be read from the Newton boundaries of  $(f, O)$  and  $(g, O)$  via toric modifications, see for instance [15, 16]. Note that the argument below can be interpreted in the context of the book of D. Eisenbud and W. Neumann [4], which is used in the proof of [17, Corollary 2.2].

The case  $p/q < r/s$  turns out to be the case  $p/q > r/s$  by exchanging  $f$  and  $g$  because of the following reason. The map  $(x, y) \mapsto (\bar{x}, \bar{y})$  does not change the orientation of  $S_\varepsilon^3$ , reverse the argument in the target of the fibration, and reverse the orientation of the fibre surface. Therefore  $f\bar{g}/|f\bar{g}| : S_\varepsilon^3 \setminus L_{f\bar{g}} \rightarrow S^1$  is a locally trivial fibration if and only if  $g\bar{f}/|g\bar{f}| : S_\varepsilon^3 \setminus L_{g\bar{f}} \rightarrow S^1$  is, and moreover if they define fibrations then their fibre surfaces are isotopic. Thus we only need to prove the case  $p/q \geq r/s$ .

The Newton boundary of  $(f\bar{g}, O)$  is as shown in Figure 2. Let  $\vec{n}_i = {}^t(\alpha_i, \beta_i)$ ,  $i = 1, \dots, N$ , be primitive vectors (i.e.,  $\gcd(\alpha_i, \beta_i) = 1$ ) which satisfy the following conditions:

- (i)  $\vec{n}_1 = {}^t(1, 0)$  and  $\vec{n}_N = {}^t(0, 1)$ ;
- (ii) the indices of  $\vec{n}_i$ 's are assigned in the counterclockwise orientation;
- (iii) there are indices  $i_f$  and  $i_g$  such that  $\vec{n}_{i_f} = {}^t(q_0, p_0)$  and  $\vec{n}_{i_g} = {}^t(s_0, r_0)$  respectively, where  $p_0 = p/\gcd(p, q)$ ,  $q_0 = q/\gcd(p, q)$ ,  $r_0 = r/\gcd(r, s)$  and  $s_0 = s/\gcd(r, s)$ ;
- (iv)  $\det(\vec{n}_i, \vec{n}_{i+1}) = 1$  for each  $i = 1, \dots, N-1$ .

For each  $\text{Cone}(\vec{n}_i, \vec{n}_{i+1})$ ,  $i = 1, \dots, N-1$ , we prepare an affine coordinate chart  $U_i$  with coordinates  $(u_i, v_i) \in U_i$  and define a birational map  $\varphi_i : U_i \rightarrow \mathbb{C}^2$  by

$$x = u_i^{\alpha_i} v_i^{\alpha_{i+1}}, \quad y = u_i^{\beta_i} v_i^{\beta_{i+1}}.$$

The birational maps  $\{\varphi_i\}$  define a well-defined gluing of the coordinate charts  $\{U_i\}$  and we obtain the map

$$\varphi : T = \bigcup_{i=1}^{N-1} U_i \rightarrow \mathbb{C},$$

which is called a *toric modification*. Each  $\vec{n}_i$ ,  $i = 2, \dots, N-1$ , corresponds to an exceptional divisor in  $T$  and we denote it by  $E_i$ . For the plane curve  $V = \{f\bar{g} = 0\}$ , the

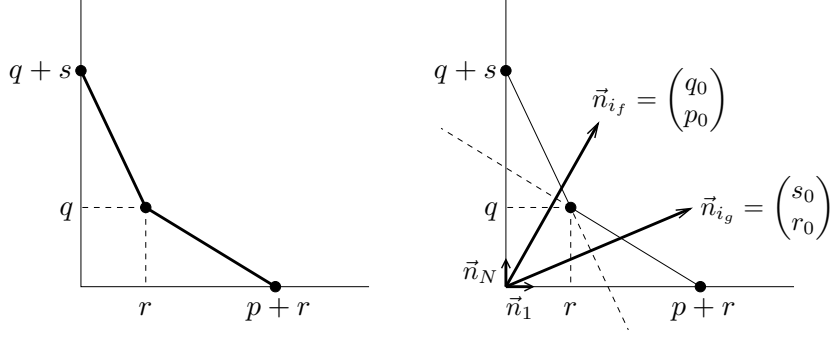


FIGURE 2. The Newton boundary of  $(f\bar{g}, O)$  in the case  $p/q > r/s$ .

closure of  $\varphi^{-1}(V \setminus \{O\})$  in  $T$  is called the *strict transform* of  $V$  and denoted by  $\tilde{V}$ . In our case,  $\tilde{V}$  becomes a smooth algebraic curve in  $T$ . In other words, the map  $\varphi : T \rightarrow \mathbb{C}$  is a resolution of the singularity  $(f\bar{g}, O)$ .

Let  $m(h, E_i)$  denote the multiplicity of a holomorphic germ  $(h, O)$  around  $E_i$ . It follows from [17, Corollary 2.2] and [18, Theorem 2.1] that  $f\bar{g}/|f\bar{g}| : S_\varepsilon^3 \setminus L_{f\bar{g}} \rightarrow S^1$  is a locally trivial fibration if and only if  $m(f, E_i) \neq m(g, E_i)$  for every  $E_i$  corresponding to a rupture vertex in the dual graph of the resolution. Here a vertex is called *rupture* if it has at least three incident edges where the arrows representing the strict transforms are considered as edges. The multiplicity  $m(h, E_i)$  of  $(h, O)$  can be read from the Newton boundary of  $(h, O)$  as

$$m(h, E_i) = \min\{\alpha_i X + \beta_i Y \mid (X, Y) \text{ is a vertex on the Newton boundary of } (h, O)\},$$

where  $\vec{n}_i = {}^t(\alpha_i, \beta_i)$  is the primitive vector corresponding to  $E_i$ . Using this formula, we have

$$\begin{aligned} m(f, E_2) &= q, \\ m(f, E_{i_g}) &= r_0 q = r q / \gcd(r, s), \\ m(f, E_{i_f}) &= q_0 p = q p / \gcd(p, q), \\ m(f, E_{N-1}) &= p, \end{aligned}$$

and

$$\begin{aligned} m(g, E_2) &= s, \\ m(g, E_{i_g}) &= r_0 s = r s / \gcd(r, s), \\ m(g, E_{i_f}) &= q_0 r = q r / \gcd(p, q), \\ m(g, E_{N-1}) &= r. \end{aligned}$$

In case (1), we have  $m(f, E_{i_g}) \neq m(g, E_{i_g})$  and  $m(f, E_{i_f}) \neq m(g, E_{i_f})$  and the other exceptional divisors are not rupture. Therefore  $f\bar{g}/|f\bar{g}| : S_\varepsilon^3 \setminus L_{f\bar{g}} \rightarrow S^1$  is a locally trivial fibration. In case (2), by the assumption  $p/q \geq r/s$ , we only need to consider the case  $p = r > 1$ ,  $q = 1$  and  $s > 1$ . We choose  $\{\vec{n}_i\}$  such that  $i_f = N - 1$  and  $\vec{n}_{i_f} = {}^t(1, p)$ . Then, in the dual graph, the vertex corresponding to  $E_{i_f}$  is not rupture. The vertex corresponding to  $E_{i_g}$  is rupture and, since  $q \neq s$ , we have  $m(f, E_{i_g}) \neq m(g, E_{i_g})$ . All other exceptional divisors are not rupture. Hence  $f\bar{g}/|f\bar{g}| : S_\varepsilon^3 \setminus L_{f\bar{g}} \rightarrow S^1$  is a locally

trivial fibration. Case (3) turns out to be case (2) by exchanging the variables  $x$  and  $y$ . In case (4),  $(f\bar{g}, O)$  is a normal crossing and the corresponding vertex in the dual graph is not rupture. Hence  $f\bar{g}/|f\bar{g}| : S_\varepsilon^3 \setminus L_{f\bar{g}} \rightarrow S^1$  is a locally trivial fibration.

Suppose  $f$  and  $g$  are not in cases (1), (2), (3) and (4). In this case, either  $E_{i_g}$  or  $E_{i_f}$  corresponds to a rupture vertex in the dual graph and satisfies  $m(f, E_{i_g}) = m(g, E_{i_g})$  or  $m(f, E_{i_f}) = m(g, E_{i_f})$  respectively. Hence  $f\bar{g}/|f\bar{g}| : S_\varepsilon^3 \setminus L_{f\bar{g}} \rightarrow S^1$  is not a locally trivial fibration. This proves the first assertion of the lemma.

Next we calculate the Euler characteristic  $\chi(F)$  of the fibre surface  $F$ . For our convenience, we choose  $\{\vec{n}_i\}$  in such a way that  $i_g > 2$  and  $i_f < N - 1$ . Note that the results of the calculations of the multiplicities above do not change even if we re-choose  $\{\vec{n}_i\}$  with these additional conditions. Set

$$E_i^\circ = E_i \setminus \left( \tilde{V} \cup \bigcup_{i \neq j} E_j \right).$$

Their Euler characteristics  $\chi(E_i^\circ)$  are given by

$$\begin{aligned} \chi(E_2^\circ) &= \chi(E_{N-1}^\circ) = 1, \\ \chi(E_{i_g}^\circ) &= -\gcd(r, s), \\ \chi(E_{i_f}^\circ) &= -\gcd(p, q), \\ \chi(E_i^\circ) &= 0 \quad \text{otherwise.} \end{aligned}$$

In the case where  $f\bar{g}/|f\bar{g}| : S_\varepsilon^3 \setminus L_{f\bar{g}} \rightarrow S^1$  is a locally trivial fibration, the Euler characteristic  $\chi(F)$  is calculated according to the technique in [1] as

$$\begin{aligned} \chi(F) &= \sum_{i=2}^{N-1} |m(f, E_i) - m(g, E_i)| \chi(E_i^\circ) \\ &= |q - s| - |rq - rs| - |qp - qr| + |p - r| \\ &= |q - s|(1 - r) + |p - r|(1 - q). \end{aligned}$$

This completes the proof of the lemma.  $\square$

#### 4. PROOF OF THEOREM 1.1

The following theorem, combined with Theorem 2.2, implies Theorem 1.1.

**Theorem 4.1.** *Let  $(f, O)$  and  $(g, O)$  be holomorphic germs given by  $f = x^p + y^q$  and  $g = x^r + y^s$  having no common branches. Suppose  $f\bar{g}/|f\bar{g}| : S_\varepsilon^3 \setminus L_{f\bar{g}} \rightarrow S^1$  is a locally trivial fibration. Then its fibre surface is not quasipositive.*

We will prove this theorem in this section. Remark that the fibre surface of  $f\bar{g}/|f\bar{g}| : S_\varepsilon^3 \setminus L_{f\bar{g}} \rightarrow S^1$  is quasipositive if and only if that of  $g\bar{f}/|g\bar{f}| : S_\varepsilon^3 \setminus L_{g\bar{f}} \rightarrow S^1$  is. So, we can exchange  $f$  and  $g$  if necessary. We can also exchange the variables  $x$  and  $y$  if necessary.

In Lemma 3.1, there are four cases (1), (2), (3) and (4) where  $f\bar{g}/|f\bar{g}| : S_\varepsilon^3 \setminus L_{f\bar{g}} \rightarrow S^1$  is a locally trivial fibration. In case (4), the fibration is topologically equivalent to  $x\bar{y}/|x\bar{y}| : S_\varepsilon^3 \setminus L_{x\bar{y}} \rightarrow S^1$ , which is the mirror image of the Milnor fibration of  $(xy, O)$ . The fibre surface of this mirror image is a negative Hopf band and it is well-known that this fibre surface is not quasipositive (for instance, use Lemma 2.3). Case (3) turns out to be

case (2) by exchanging the variables  $x$  and  $y$ . In case (2), we can assume that  $p = r$  and  $q = 1$  by exchanging  $f$  and  $g$  if necessary. In particular,  $p/q > r/s$ ,  $p/q > 1$  and  $q \neq s$ . In case (1), we can assume  $p/q \geq 1$  by exchanging the variables  $x$  and  $y$  if necessary. If  $p/q < r/s$  then  $p/q \geq 1$  implies  $r/s > 1$ . Thus, the case  $p/q < r/s$  turns out to be the case  $p/q > r/s$  by exchanging  $f$  and  $g$  with keeping the assumption  $p/q \geq 1$ . Thus it is enough to prove the assertion in cases (1) and (2) under the assumptions  $p/q \geq r/s$ ,  $p/q \geq 1$  and  $q \neq s$ .

We here present the plan of the proof.

(A)  $p \geq r$

(A-1)  $q \leq r$

We prove this case in Section 4.1.

(A-2)  $q > r$

We prove this case in Section 4.2.

(B)  $p < r$

This case happens only in case (1). If  $r/s \leq 1$  then  $s \geq r > p \geq q$ . In this case, by exchanging  $x$  and  $y$  and also  $f$  and  $g$ , it turns out to be case (A). So, we can assume that  $r/s > 1$ . Since  $p/q \geq r/s$  and  $p < r$ , we have the inequality  $q < s$ .

We prove this case in Section 4.3.

In the proof, we need to present the position of the fibre surface. In order to describe the position, we will use the following braid foliation. Let  $\Theta : S_\varepsilon^3 \setminus \{y = 0\} \rightarrow S^1$  be the fibration given by  $\Theta((x, y)) = \arg y$ . The fibred link is the trivial knot  $S_\varepsilon^3 \cap \{y = 0\}$  and the fibre surface is a half-plane  $H_\theta = \{(x, y) \in S_\varepsilon^3 \mid \arg y = \theta\}$ , where  $\theta \in S^1$ . For the holomorphic function  $f(x, y) = x^p + y^q$ , the link  $S_\varepsilon^3 \cap L_f$  is determined by  $x = (-y^q)^{1/p}$ . The link  $L_f$  intersects  $H_\theta$  transversely and, on each  $H_\theta$ , these intersection points lie on a circle  $C_f$  centered at  $H_\theta \cap \{x = 0\}$ . The number of these intersection points is called a *braid index*. The braid index of  $L_f$  with respect to  $H_\theta$  is  $p$ . Also, the intersection points of  $L_g$  with  $H_\theta$  lie on a circle  $C_g$  centered at  $H_\theta \cap \{x = 0\}$  and its braid index is  $r$ . Since  $S_\varepsilon^3$  is sufficiently small, we can assume that  $|y| < 1$ . In the case  $p/q > r/s$ ,  $x = (-y^s)^{1/r}$  is closer to  $x = 0$  than  $x = (-y^q)^{1/p}$ , that is,  $C_g$  lies inside  $C_f$ , see on the left in Figure 3. In the case  $p/q = r/s$ ,  $C_f$  coincides with  $C_g$ , though we also use the positions in Figure 3 to distinguish these circles. In the proof, for convenience, we align the intersection points of  $L_f$  and  $L_g$  with  $H_\theta$  vertically as shown on the right in Figure 3.

Using the braid foliation, a Seifert surface  $S$  bounded by the link  $L_{f\bar{g}}$  is represented as the move of the intersection  $S \cap H_\theta$  for  $\theta \in S^1$ . Setting  $S$  in a good position, we assume that  $S$  is tangent to  $H_\theta$  only at a finite number of saddles. A saddle appears during the move of  $S \cap H_\theta$  as shown in Figure 4.

**4.1. Case (A-1).** To describe the Seifert surface  $S$ , we first prepare the section  $S \cap H_\theta$  at  $\theta = 0$ . There are  $p$  intersection points  $a_1, a_2, \dots, a_p$  of  $L_f \cap H_0$  on  $C_f$  and  $r$  intersection points  $b_{p-r+1}, b_{p-r+2}, \dots, b_p$  of  $L_g \cap H_0$  on  $C_g$ . We connect  $a_i$  and a point  $e_i$  on the axis  $\{y = 0\}$  by a horizontal interval  $C(a_i, e_i)$  for each  $i = 1, \dots, p - r$  and connect  $a_i$  and  $b_i$  by a horizontal interval  $C(a_i, b_i)$  for each  $i = p - r + 1, \dots, p$  as shown in Figure 5 (a). The figure represents the case  $p = 8$  and  $r = 5$ . The dotted curve  $R$  connecting the center  $x = 0$  and the axis  $\{y = 0\}$  is used to refer how many times the intersection points  $L_{f\bar{g}} \cap H_\theta$  rotate around  $x = 0$ .

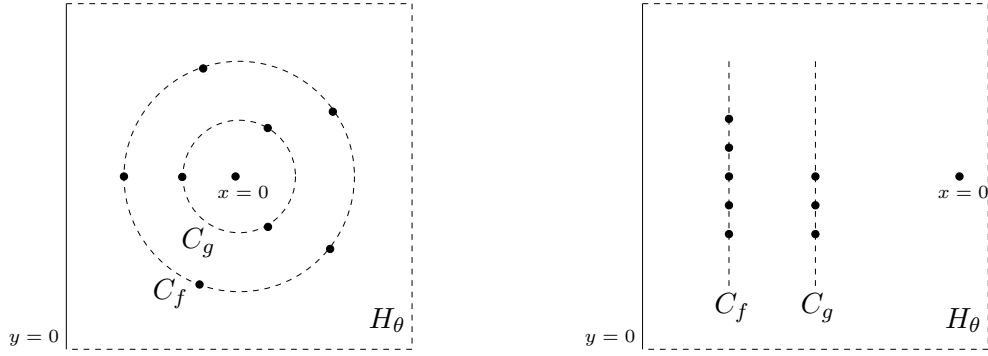


FIGURE 3. The intersection points of  $L_f$  and  $L_g$  with  $H_\theta$ . The figures are in the case  $p = 5$  and  $r = 3$ .

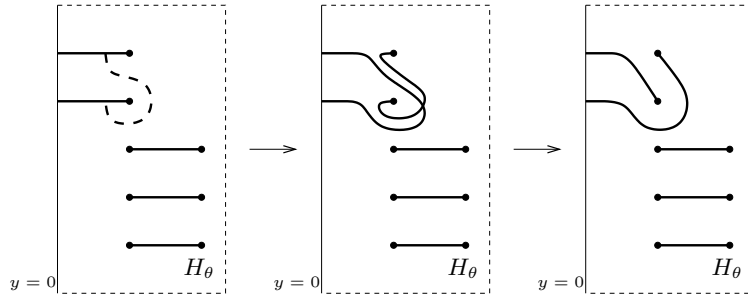


FIGURE 4. An example of a saddle appearing in the move of  $S \cap H_\theta$ .

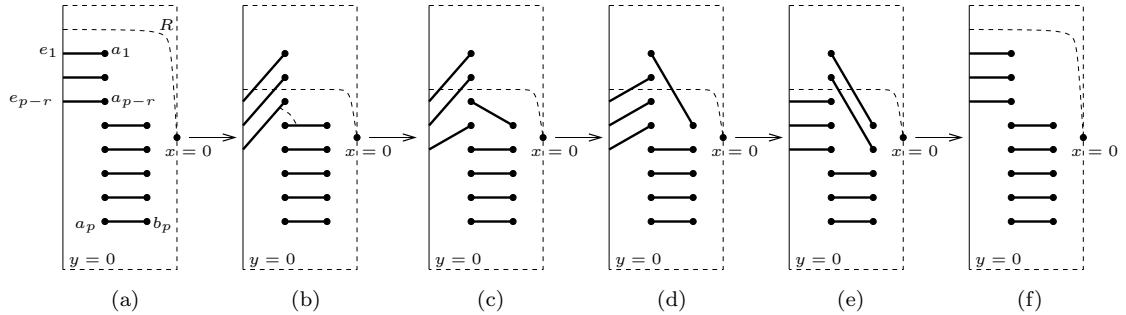


FIGURE 5. The move of intervals on  $H_\theta$  in case (A-1) with  $q \leq p - r$ .

As  $\theta$  changes from 0 to  $2\pi$ , the  $p$  points on  $C_f$  move round  $C_f$   $q/p$  times in the clockwise orientation. Instead of moving these points, we move the reference-curve  $R$   $q/p$  times around  $x = 0$  in the counterclockwise orientation with keeping the points  $e_1, \dots, e_{p-r}$  on  $\{y = 0\}$  under  $R$ . The moved reference-curve  $R$  passes between  $a_q$  and  $a_{q+1}$ .

In the case  $q \leq p - r$ , the reference-curve  $R$  passes over  $b_{p-r+1}$ . This case is shown in Figure 5 (b). The figure represents the case  $q = 2$ . We next apply a saddle between  $C(a_{p-r}, e_{p-r})$  and  $C(a_{p-r+1}, b_{p-r+1})$ . The dotted arc in Figure 5 (b) represents the position of the saddle and we obtain Figure 5 (c). By applying  $p - r - 1$  saddles further, we obtain Figure 5 (d). We then repeat the same process for the intervals  $C(a_i, b_i)$  for  $i = p - r + 2, \dots, p - r + q$  (here we do nothing in the case  $q = 1$ ) and obtain Figure 5 (e).

During the process from (a) to (e), we applied totally  $(p-r)q$  saddles. By moving the points  $b_{p-r+1}, \dots, b_{p-r+q}$  round  $C_g$   $q/r$  times, we obtain Figure 5 (f).

The move of the intervals in the case  $q > p-r$  is shown in Figure 6. The figure represents the case  $q = 4$ . The difference from the case  $q \leq p-r$  is only the position of the reference-curve  $R$ . So, in this case, we also use  $(p-r)q$  saddles.

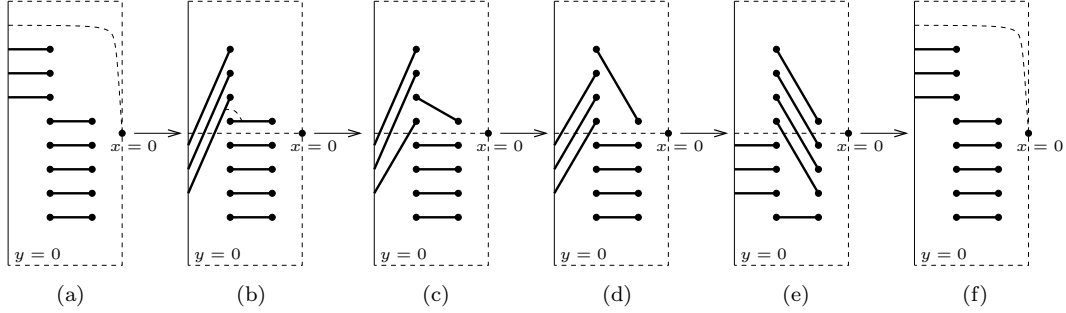


FIGURE 6. The move of intervals on  $H_\theta$  in case (A-1) with  $q > p-r$ .

In both cases, the points on  $C_g$  have been moved round  $C_g$   $q/r$  times. Hence we need to move them further  $(s-q)/r$  times in the clockwise direction if  $s > q$  and  $(q-s)/r$  times in the counterclockwise direction if  $s < q$ . Figure 7 (f)-(g)-(h)-(a') represents the  $1/r$ -rotation in the case  $s > q$  and Figure 7 (g') represents the first step of the  $1/r$ -rotation in the case  $s < q$ . We repeat this process  $|q-s|$  times, where we use  $|s-q|(r-1)$  saddles, and complete the necessary move. Since the configuration of the intervals in Figure 7 (a') is the same as those in Figure 5 (a) and Figure 6 (a), this move of intervals on  $H_\theta$  constitutes a surface  $S$  in  $S_\varepsilon^3$  bounded by the link  $L_{f\bar{g}}$ . It is easy to check that this surface is a Seifert surface. In [17, Proposition 3.1], Pichon proved that if the orientation of the link components  $L_f$  induced by the fibre surface is consistent with the parameter  $\theta$  then that of  $L_g$  is opposite to  $\theta$ . It is easy to verify that the orientation of  $L_{f\bar{g}}$  induced by  $S$  satisfies this property.

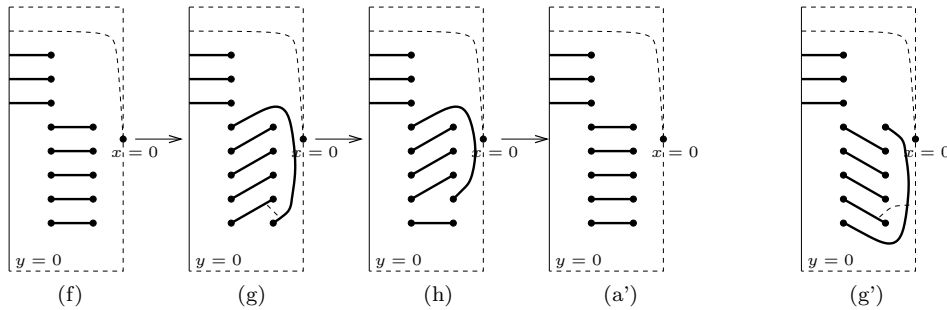


FIGURE 7. The move of intervals during the  $1/r$ -rotation of  $L_{\bar{g}} \cap H_\theta$  in case (A-1).

**Lemma 4.2.**  *$S$  is ambient isotopic to the fibre surface  $F$  in case (A-1).*

*Proof.* The surface  $S$  is obtained from  $p-r$  disks and a number of annuli by attaching bands corresponding to the saddles. Therefore the Euler characteristic  $\chi(S)$  of  $S$  is given

by

$$\chi(S) = (p-r) - (p-r)q - |s-q|(r-1) = |p-r|(1-q) + |q-s|(1-r),$$

which coincides with  $\chi(F)$  in Lemma 3.1. It is well-known that the fibration of an oriented fibred link is unique up to isotopy and that all minimal genus Seifert surfaces of a fibred link are ambient isotopic to the fibre surface, see for instance [4, p. 34] or [10, Theorem 4.1.10]. Thus we can conclude that  $F$  is ambient isotopic to  $S$ .  $\square$

*Proof of Theorem 1.1 in case (A-1).* By Lemma 2.3 and Lemma 4.2, it is enough to show the existence of an essential, simple closed curve  $\gamma$  on  $S$  which is a trivial knot in  $S_\varepsilon^3$  and satisfies  $\ell(\gamma, S) \leq 0$ . We present such a  $\gamma$  by using the move of the section  $\gamma \cap H_\theta$  for  $\theta \in S^1$ . Set  $\gamma \cap H_0$  to be a point on the interval  $C(a_{p-r+1}, b_{p-r+1})$  whose position is represented by a white box in Figure 8 (a). In the case  $s > q$ , the position of  $\gamma$  can be seen in Figure 8 by following the white box. Note that the move from (f) to (g) always occur since  $s > q$ . In the case  $|s-q| \geq 2$ , after the first  $1/r$ -rotation of  $L_{\bar{g}} \cap H_\theta$  from (f) to (a'), we keep  $\gamma \cap H_\theta$  on the interval connected to  $a'$  described in Figure 8 (a'). The obtained  $\gamma$  is obviously a trivial knot in  $S_\varepsilon^3$ . We can prove that  $\gamma$  is essential in  $S$  as follows. Assume  $\gamma$  bounds a disk in  $S$ . Even if we cut  $S$  by arcs  $\delta_1, \dots, \delta_k$  in  $S \setminus \gamma$  whose endpoints lie on the boundary of  $S$ ,  $\gamma$  still bounds a disk in the connected component of  $S \setminus \bigcup_{i=1}^k \delta_i$  containing  $\gamma$ . However, in our case, we can cut  $S$  in such a way that the connected component containing  $\gamma$  is an annulus whose core curve is  $\gamma$ . Therefore, it does not bound a disk in  $S$ . It is also easy to check that  $\ell(\gamma, S) = 0$ , which proves the assertion in this case.

In the case  $s < q$ , we can find a curve  $\gamma$  which is essential in  $S$ , a trivial knot in  $S_\varepsilon^3$ , and satisfies  $\ell(\gamma, S) = -1$  in a similar way. This completes the proof.  $\square$

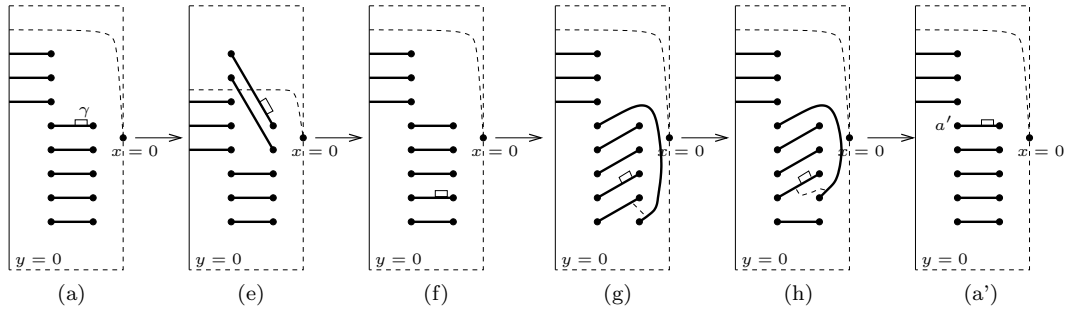


FIGURE 8. The simple closed curve  $\gamma$  on  $S$  in the case  $s > q$ .

**4.2. Case (A-2).** The Seifert surface  $S$  in this case is described in Figure 9, which represents the case  $p = 8$  and  $r = 2$ . We set the section  $S \cap H_0$  as before. In the case  $q \leq p - r$ , we move the reference-curve  $R$   $q/p$  times in the counterclockwise direction. Figure 9 (b) represents the case  $q = 3$ . Then, by applying  $(p-r)r$  saddles, we obtain Figure 9 (c). Moving the intersection points  $b_{p-r+1}, \dots, b_p$  around  $x = 0$  in the clockwise orientation, we obtain Figure 9 (d). If  $q - r > r$  then we need to iterate the move from (b) to (d)  $\lfloor (q-r)/r \rfloor$  times. After these moves, we have the situation where there are  $(q \bmod r)$  intersection points on  $C_f$  over  $R$ . Then apply saddles further  $(p-r)(q \bmod r)$  times and obtain Figure 9 (e). We used totally  $(p-r)r \lfloor q/r \rfloor + (p-r)(q \bmod r) = (p-r)q$

saddles. Finally, by moving the top  $(q \bmod r)$  intervals connecting two points on  $C_f$  and  $C_g$  around  $x = 0$  in the clockwise orientation, we obtain Figure 9 (f). The move after this figure is exactly the same as in case (A-1) shown in Figure 7 and we use  $|s - q|(r - 1)$  saddles. The move of the intervals in the case  $q > p - r$  is analogous to the case  $q \leq p - r$  as in case (A-1). In both cases, the move of intervals on  $H_\theta$  constitutes a surface  $S$  in  $S_\varepsilon^3$  bounded by the link  $L_{f\bar{g}}$  and it is easy to check that  $S$  is a Seifert surface and that the orientation on the boundary of  $S$  is consistent with the orientation of  $L_{f\bar{g}}$ .

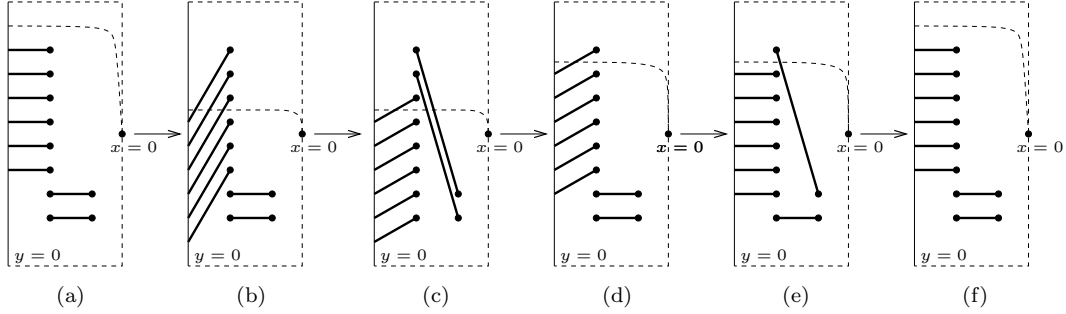


FIGURE 9. The move of intervals on  $H_\theta$  in case (A-2).

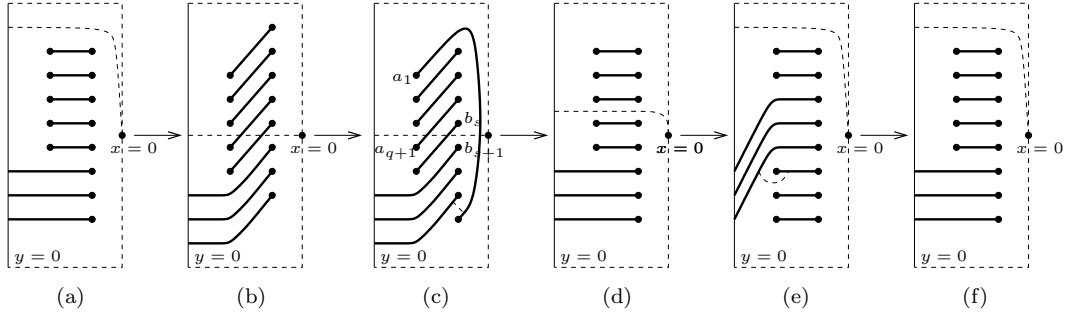
**Lemma 4.3.**  *$S$  is ambient isotopic to the fibre surface  $F$  in case (A-2).*

*Proof.* The assertion follows from the same argument as in the proof of Lemma 4.2.  $\square$

*Proof of Theorem 1.1 in case (A-2).* As in the proof in case (A-1), we will show the existence of  $\gamma$  which is essential in  $S$ , a trivial knot in  $S_\varepsilon^3$ , and satisfies  $\ell(\gamma, S) \leq 0$ . We set  $\gamma \cap H_0$  to be a point on the interval  $C(a_{p-r+1}, b_{p-r+1})$  and keep it on the interval connected to  $b_{p-r+1}$  until Figure 9 (d). Since the move from (b) to (d) is iterated  $\lfloor q/r \rfloor$  times, the section of  $\gamma$  is full-twisted  $\lfloor q/r \rfloor$  times in the clockwise direction in this part. The move of  $\gamma \cap H_\theta$  in the rest is the same as in case (A-1). Hence we have  $\ell(\gamma, S) = -\lfloor q/r \rfloor$  in the case  $s > q$  and  $\ell(\gamma, S) = -\lfloor q/r \rfloor - 1$  in the case  $s < q$ . Since  $q > r$  by the assumption,  $\gamma$  satisfies  $\ell(\gamma, S) < 0$ . It is easy to check that  $\gamma$  is a trivial knot in  $S_\varepsilon^3$  and essential in  $S$ . This completes the proof.  $\square$

**4.3. Case (B).** The Seifert surface  $S$  in this case is described in Figure 10. The section  $L_{f\bar{g}} \cap H_0$  consists of  $p$  points  $a_1, \dots, a_p$  on  $C_f$  and  $r$  points  $b_1, \dots, b_r$  on  $C_g$ . We connect  $a_i$  and  $b_i$  by a horizontal interval  $C(a_i, b_i)$  for each  $i = 1, \dots, p$  and connect  $b_i$  and a point  $e_i$  on the axis  $\{y = 0\}$  by a horizontal interval  $C(e_i, b_i)$  for each  $i = p+1, \dots, r$  as shown in Figure 10 (a). The figure represents the case  $p = 5$  and  $r = 8$ .

As  $\theta$  changes from 0 to  $2\pi$ , the  $p$  points on  $C_f$  move round  $C_f$   $q/p$  times and the  $r$  points on  $C_g$  move round  $C_g$   $s/r$  times in the clockwise orientation. Here we remind that we have the assumptions  $p/q \geq 1$ ,  $r/s > 1$  and  $q < s$ . Instead of these moves, we move the reference-curve  $R$  in the counterclockwise orientation. Then the curve  $R$  passes between  $a_q$  and  $a_{q+1}$  if  $p > q$  and just under  $a_q$  if  $p = q$ . For  $C_g$ , it passes between  $b_s$  and  $b_{s+1}$ . This is shown in Figure 10 (b), which is in the case  $q = 3$  and  $s = 5$ . The figures (b) and (c) represent the same configuration. We next apply a saddle in the position represented by the dotted arc in Figure 10 (c). We iterate the same kind of saddles totally  $(r - 1)(s - q)$

FIGURE 10. The move of intervals on  $H_\theta$  in case (B).

times and obtain Figure 10 (d). The figures (d) and (e) represent the same configuration. We then apply a saddle in the position represented by the dotted arc in Figure 10 (e), iterate the same kind of saddles totally  $(r - p)q$  times and obtain Figure 10 (f). The configuration of the intervals in Figure 10 (f) is the same as that in Figure 10 (a) and hence this move of intervals on  $H_\theta$  constitutes a surface  $S$  in  $S_\varepsilon^3$  bounded by the link  $L_{f\bar{g}}$ . It is easy to check that  $S$  is a Seifert surface and that the orientation on the boundary of  $S$  is consistent with the orientation of  $L_{f\bar{g}}$ .

**Lemma 4.4.**  $S$  is ambient isotopic to the fibre surface  $F$  in case (B).

*Proof.* The assertion follows from the same argument as in the proof of Lemma 4.2.  $\square$

*Proof of Theorem 1.1 in case (B).* As in the proofs in case (A), we will show the existence of  $\gamma$  which is essential in  $S$ , a trivial knot in  $S_\varepsilon^3$ , and satisfies  $\ell(\gamma, S) \leq 0$ . We set  $\gamma \cap H_0$  to be a point on the interval  $C(a_1, b_1)$ . The section of  $\gamma$  stays at this position until we have the saddle between  $C(a_1, b_{s+1})$  and  $C(a', b_s)$  in the process between (c) and (d), where  $a' = a_{q+1}$  in the case  $p > q$  and  $a' = e_{q+1}$  in the case  $p = q$ . Using this saddle, we shift the section of  $\gamma$  onto the interval  $C(a', b_{s+1})$  and, after that, keep it on the interval connected to  $b_{s+1}$ . This move defines a simple closed curve  $\gamma$  on  $S$ , which is a trivial knot in  $S_\varepsilon^3$ , essential in  $S$ , and satisfies  $\ell(\gamma, S) = 0$ . Thus we have the assertion.  $\square$

## 5. NEWTON NON-DEGENERATE CASE

Let  $(f, O)$  and  $(g, O)$  be holomorphic germs at  $O \in \mathbb{C}^2$ . If the Newton boundaries of  $(f, O)$  and  $(g, O)$  are Newton non-degenerate, the topological types of these singularities are determined by their Newton boundaries, see [14]. Therefore we can easily generalize the statements of Theorem 1.1 and Corollary 1.2.

**Corollary 5.1.** *Suppose that  $(f, O)$  and  $(g, O)$  are Newton non-degenerate holomorphic germs whose Newton boundaries are the same as those of  $(x^p + y^q, O)$  and  $(x^r + y^s, O)$  respectively. Suppose either*

- (1)  $p \neq r$  and  $q \neq s$ ,
- (2)  $p = r > 1$ ,  $q \neq s$  and  $\min\{q, s\} = 1$ ,
- (3)  $p \neq r$ ,  $q = s > 1$  and  $\min\{p, r\} = 1$ , or
- (4) at least three of  $p, q, r, s$  are 1.

In the case  $p/q = r/s$ , assume further that the Newton boundary of  $(fg, O)$  is non-degenerate. Then  $f\bar{g}/|f\bar{g}| : S_\varepsilon^3 \setminus L_{f\bar{g}} \rightarrow S^1$  is a locally trivial fibration and the fibre surface is not quasipositive. As a consequence, the compatible contact structure is overtwisted and the monodromy contains at least one negative Dehn twist.

*Proof.* The resolution graph of  $(f\bar{g}, O)$  is the same as that of  $((x^p + y^q)\overline{(x^r + y^s)}, O)$ . Hence the argument in Section 3 shows that  $f\bar{g}/|f\bar{g}| : S_\varepsilon^3 \setminus L_{f\bar{g}} \rightarrow S^1$  is a locally trivial fibration. Since  $L_{fg}$  is ambient isotopic to the link of  $((x^p + y^q)(x^r + y^s), O)$ ,  $L_{f\bar{g}}$  is ambient isotopic to the link of  $((x^p + y^q)\overline{(x^r + y^s)}, O)$ . Hence the surface  $S$  described in Section 4 is the fibre surface of the fibration in this case also, which is not quasipositive.  $\square$

**Corollary 5.2.** *Let  $(f, O)$  and  $(g, O)$  be holomorphic germs such that  $f = x$  and  $(g, O)$  is Newton non-degenerate whose Newton boundary is the same as that of  $(x^p + y^q, O)$ . Then  $f\bar{g}/|f\bar{g}| : S_\varepsilon^3 \setminus L_{f\bar{g}} \rightarrow S^1$  is a locally trivial fibration and the fibre surface is not quasipositive. As a consequence, the compatible contact structure is overtwisted and the monodromy contains at least one negative Dehn twist.*

*Proof.* By the change of coordinates  $(x, y) \mapsto (x + y^{q+1}, y)$ , the germ  $(f\bar{g}, O)$  can be replaced by a germ which is Newton non-degenerate and whose Newton boundary is the same as that of  $((x + y^{q+1})\overline{(x^p + y^q)}, O)$ . Hence, by Corollary 5.1,  $f\bar{g}/|f\bar{g}| : S_\varepsilon^3 \setminus L_{f\bar{g}} \rightarrow S^1$  is a locally trivial fibration and the fibre surface is not quasipositive.  $\square$

## 6. REAL ANALYTIC GERMS $xy\overline{(x^p + y^q)}$

In this last section, we consider the case where  $f = xy$  and  $g = x^p + y^q$ ,  $p, q \in \mathbb{N}$ . If  $p$  and  $q$  do not satisfy  $p = q = 2$ , then the Newton boundary of  $(g, O)$  does not contain the point  $(1, 1)$ , which is the Newton boundary of  $(f, O)$ . Therefore, using [17, Corollary 2.2] and [18, Theorem 2.1], we conclude that  $f\bar{g}/|f\bar{g}| : S_\varepsilon^3 \setminus L_{f\bar{g}} \rightarrow S^1$  is a locally trivial fibration. In the case  $p = q = 2$ , the vertex in the dual graph corresponding to the exceptional divisor  $E_{i_g}$  is rupture and  $m(f, E_{i_g}) = m(g, E_{i_g})$ . Hence [17, Corollary 2.2] shows that  $f\bar{g}/|f\bar{g}| : S_\varepsilon^3 \setminus L_{f\bar{g}} \rightarrow S^1$  is not a locally trivial fibration.

If it is a fibration, we have the same conclusion as in Theorem 1.1.

**Theorem 6.1.** *Let  $(f, O)$  and  $(g, O)$  be holomorphic germs given by  $f = xy$  and  $g = x^p + y^q$ . Suppose  $f\bar{g}/|f\bar{g}| : S_\varepsilon^3 \setminus L_{f\bar{g}} \rightarrow S^1$  is a locally trivial fibration. Then the fibre surface is not quasipositive and, as a consequence, the compatible contact structure is overtwisted and the monodromy contains at least one negative Dehn twist.*

We first determine the Euler characteristic of the fibre surface.

**Lemma 6.2.** *Let  $(f, O)$  and  $(g, O)$  be holomorphic germs given by  $f = xy$  and  $g = x^p + y^q$ . Suppose  $f\bar{g}/|f\bar{g}| : S_\varepsilon^3 \setminus L_{f\bar{g}} \rightarrow S^1$  is a locally trivial fibration. Then the Euler characteristic  $\chi(F)$  of the fibre surface  $F$  is given by  $\chi(F) = -|pq - p - q|$ .*

*Proof.* The Euler characteristic  $\chi(F)$  can be read from the Newton boundary as in Section 3. Since  $f = xy$ ,  $\vec{n}_1$  and  $\vec{n}_N$  also correspond to exceptional divisors  $E_1$  and  $E_N$  in  $T$  respectively and hence we have  $\chi(E_j^\circ) = 0$  for  $j \neq i_g$ . For  $E_{i_g}$ , we have  $\chi(E_{i_g}^\circ) = -\gcd(p, q)$ ,  $m(g, E_{i_g}) = pq/\gcd(p, q)$  and  $m(xy, E_{i_g}) = q/\gcd(p, q) + p/\gcd(p, q)$ . Hence  $\chi(F)$  is given

by

$$\chi(F) = \left| \frac{pq}{\gcd(p, q)} - \left( \frac{q}{\gcd(p, q)} + \frac{p}{\gcd(p, q)} \right) \right| (-\gcd(p, q)) = -|pq - p - q|.$$

□

*Proof of Theorem 6.1.* In the case  $p, q \geq 2$ , we prove the assertion by presenting a Seifert surface  $S$  in  $S^3$  bounded by  $L_{f_{\bar{g}}}$  with  $\chi(S) = \chi(F)$ , using the braid foliation as in Section 4. In this case  $\{x = 0\}$  and  $\{y = 0\}$  are components of the link  $L_{f_{\bar{g}}}$ . The component  $\{y = 0\}$  is vertical in Figure 3, which is not useful for us. So, we perturb it very little so that it is transverse to  $H_\theta$  for  $\theta \in S^1$ . We set the section  $S \cap H_0$  as shown in Figure 11 (a), where the  $p$  points aligned vertically in the middle are the section  $L_{\bar{g}} \cap H_0$ . As  $\theta$  changes from 0 to  $2\pi$ , the  $p$  points in the middle move around  $x = 0$   $q/p$  times in the clockwise orientation and the point close to the axis  $\{y = 0\}$  moves around  $x = 0$  once in the same direction.

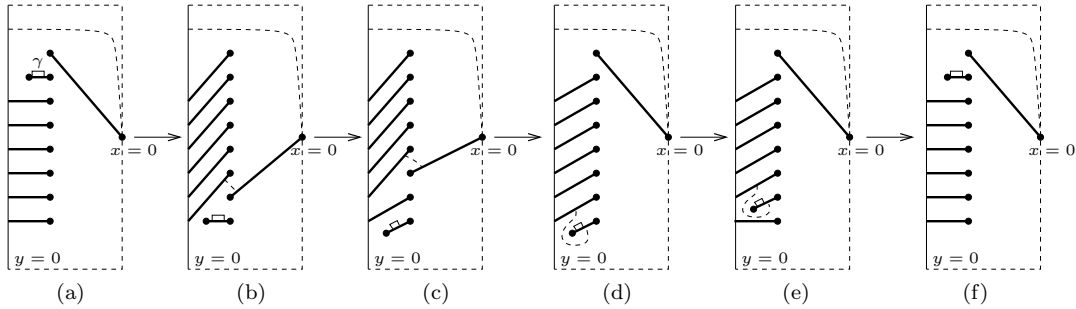


FIGURE 11. The move of intervals on  $H_\theta$  in the case  $q = 2$ . The figures are in the case  $p = 8$ .

Figure 11 represents the move of section  $S \cap H_\theta$  in the case  $q = 2$ . During the move from (a) to (b), the  $p$  points in the middle move around  $x = 0$   $2/p$  times in the clockwise orientation. During the process from (b) to (f), we attach totally  $2(p - 2)$  saddles. This means that the surface  $S$  is obtained from  $p - 2$  disks and two annuli by attaching  $2(p - 2)$  bands. Hence

$$\chi(S) = (p - 2) - 2(p - 2) = -p + 2,$$

which coincides with  $-(pq - p - q)$  with  $q = 2$ . Thus, by Lemma 6.2, we have  $\chi(S) = \chi(F)$ .

Figure 12 represents a move from Figure 11 (b) to itself, during which the  $p$  points in the middle move around  $x = 0$   $1/p$  times. We attach  $p - 1$  saddles in this process. In the case  $q > 2$ , we repeat this process  $q - 2$  times at Figure 11 (b). Hence

$$\chi(S) = (p - 2) - (2(p - 2) + (p - 1)(q - 2)) = -(pq - p - q)$$

and, by Lemma 6.2, we have  $\chi(S) = \chi(F)$ .

The equality  $\chi(S) = \chi(F)$  implies, as Lemma 4.2, that  $S$  is ambient isotopic to  $F$ . Moreover, the move of the white box in Figure 11 and Figure 12 represents the section of an essential, simple closed curve  $\gamma$  on  $S$  which is a trivial knot in  $S_\varepsilon^3$  and satisfies  $\ell(\gamma, S) < 0$ . Hence, by Lemma 2.3, we have the assertion in the case  $p, q \geq 2$ .

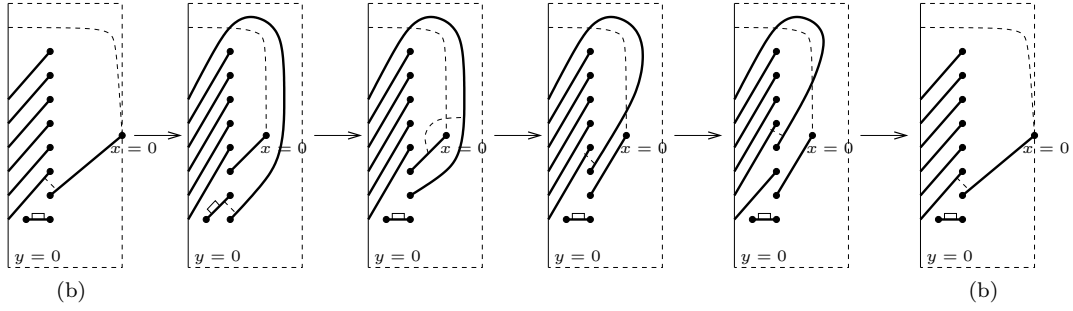


FIGURE 12. The additional move of the intervals on  $H_\theta$  in the case  $q > 2$ . The figures are in the case  $p = 8$ .

In the case where one of  $p$  and  $q$  is 1, say  $p = 1$ , the link  $L_{f\bar{g}}$  is as shown in Figure 13 and it is known in [12] that this surface is the fibre surface of  $L_{f\bar{g}}$ . By Lemma 2.3 this surface is not quasipositive and hence we have the assertion.  $\square$

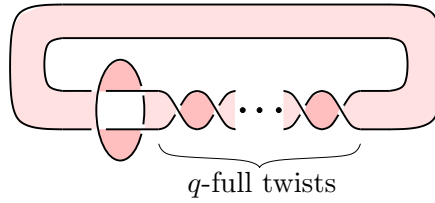


FIGURE 13. The fibre surface in the case  $p = 1$  and  $q \geq 1$ .

**Corollary 6.3.** *Let  $(f, O)$  and  $(g, O)$  be holomorphic germs such that  $f = xy$  and  $(g, O)$  is Newton non-degenerate whose Newton boundary is the same as that of  $(x^p + y^q, O)$ . Suppose that  $p$  and  $q$  do not satisfy  $p = q = 2$ . Then  $f\bar{g}/|f\bar{g}| : S_\epsilon^3 \setminus L_{f\bar{g}} \rightarrow S^1$  is a locally trivial fibration and the fibre surface is not quasipositive. As a consequence, the compatible contact structure is overtwisted and the monodromy contains at least one negative Dehn twist.*

*Proof.* The proof is the same as that of Corollary 5.1.  $\square$

## REFERENCES

- [1] N. A'Campo, *La fonction zêta d'une monodromie*, Comment. Math. Helv. **50** (1975), 233–248.
- [2] S. Baader, M. Ishikawa, *Legendrian graphs and quasipositive diagrams*, preprint, available at: arXiv.math.GT/0609592.
- [3] A. Bodin, A. Pichon, *Meromorphic functions, bifurcation sets and fibred multilinks*, Math. Res. Lett. **14** (2007), no. 3, 413–422.
- [4] D. Eisenbud, W. Neumann, *Three-dimensional link theory and invariants of plane curve singularities*, Ann. Math. Studies 110, Princeton Univ. Press, Princeton, 1985.
- [5] Y. Eliashberg, *Classification of overtwisted contact structures on 3-manifolds*, Invent. Math. **98** (1989), 623–637.
- [6] Y. Eliashberg, *Filling by holomorphic discs and its applications*, Geometry and Low-Dimensional Manifolds, 2 (Durham, 1989), London Math. Soc. Lecture Note Series **151**, Cambridge Univ. Press, Cambridge, 1990, pp. 45–67.

- [7] Y. Eliashberg, *Contact 3-manifolds twenty years since J. Martinet's work*, Ann. Inst. Fourier **42** (1992), 165–192.
- [8] E. Giroux, *Géométrie de contact: de la dimension trois vers les dimensions supérieures*, Proceedings of the International Congress of Mathematicians, Vol II (Beijing, 2002), Higher Ed. Press, Beijing, 2002, pp. 405–414.
- [9] M. Hedden, *Notions of positivity and the Ozsváth-Szabó concordance invariant*, preprint, available at: arXiv.math.GT/0509499.
- [10] A. Kawauchi, *A survey of knot theory*, Birkhäuser, Basel, 1996.
- [11] A. Loi, R. Piergallini, *Compact Stein surfaces with boundary as branched covers of  $B^4$* , Invent. Math. **143** (2001), 325–348.
- [12] P.M. Melvin, H.R. Morton, *Fibred knots of genus 2 formed by plumbing Hopf bands*, J. London Math. Soc. **34** (1986), 159–168.
- [13] J. Milnor, *Singular Points of Complex Hypersurfaces*, Ann. Math. Studies 61, Princeton Univ. Press, Princeton, 1968.
- [14] M. Oka, *On the bifurcation of the multiplicity and topology of the Newton boundary*, J. Math. Soc. Japan **31** (1979), 435–450.
- [15] M. Oka, *Geometry of plane curves via toroidal resolution*, Singularities and Algebraic Geometry (La Rábida, 1991), Progress in Mathematics 134, Birkhäuser, Basel, 1996, pp. 95–121.
- [16] M. Oka, *Non-degenerate Complete Intersection Singularities*, Hermann, Paris, 1997.
- [17] A. Pichon, *Real analytic germs  $f\bar{g}$  and open-book decompositions of the 3-sphere*, International J. Math. **16** (2005), 1–12.
- [18] A. Pichon, J. Seade, *Fibered multilinks and real singularities  $f\bar{g}$* , preprint, available at: arXiv.math.AG/0505312.
- [19] L. Rudolph, *Algebraic functions and closed braids*, Topology **22** (1983), 191–201.
- [20] L. Rudolph, *A characterization of quasipositive Seifert surface (Constructions of quasipositive knots and links, III)*, Topology **31** (1992), 231–237.
- [21] L. Rudolph, *An obstruction to sliceness via contact geometry and "classical" gauge theory*, Invent. Math. **119** (1995), 155–163.
- [22] L. Rudolph, *Quasipositive pretzels*, Topology Appl. **115** (2001), 115–123.
- [23] J. Seade, *On the topology of isolated singularities in analytic spaces*, Progress in Mathematics 241, Birkhäuser, Basel, 2006.
- [24] W.P. Thurston, H. Winkelnkemper, *On the existence of contact forms*, Proc. Amer. Math. Soc. **52** (1975), 345–347.

DEPARTMENT OF MATHEMATICS, TOKYO INSTITUTE OF TECHNOLOGY, 2-12-1, OH-OKAYAMA, MEGURO-KU, TOKYO, 152-8551, JAPAN

*E-mail address:* ishikawa@math.titech.ac.jp